AGU PUBLICATIONS

Geophysical Research Letters

RESEARCH LETTER
10.1002/2016GL070718

Key Points:
- Freshwater fluxes from melting ice melange vary with submerged ice area and area-averaged melt rate and can exceed 1000 m^3/s
- Ice melange meltwater fluxes can dominate the freshwater budget of glacial fjords throughout the majority of the year
- Solid freshwater fluxes to the open ocean cannot be estimated from glacier discharge because up to 50% of iceberg mass is melted in fjords

Supporting Information:
- Supporting Information S1
- Table S1

Correspondence to:
E. M. Enderlin,
ellyn.enderlin@gmail.com

Citation:
Enderlin, E. M., G. S. Hamilton, F. Straneo, and D. A. Sutherland (2016), Iceberg meltwater fluxes dominate the freshwater budget in Greenland's iceberg-congested glacial fjords, *Geophys. Res. Lett.*, *43*, 11,287–11,294, doi:10.1002/2016GL070718.

Received 3 AUG 2016
Accepted 24 OCT 2016
Accepted article online 26 OCT 2016
Published online 9 NOV 2016

Iceberg meltwater fluxes dominate the freshwater budget in Greenland's iceberg-congested glacial fjords

Ellyn M. Enderlin[1,2], Gordon S. Hamilton[1,2], Fiammetta Straneo[3], and David A. Sutherland[4]

[1]Climate Change Institute, University of Maine, Orono, Maine, USA, [2]School of Earth and Climate Science, University of Maine, Orono, Maine, USA, [3]Department of Physical Oceanography, Woods Hole Oceanographic Institution, Woods Hole, Massachusetts, USA, [4]Department of Geological Sciences, University of Oregon, Eugene, Oregon, USA

Abstract Freshwater fluxes from the Greenland ice sheet have increased over the last two decades due to increases in liquid (i.e., surface and submarine meltwater) and solid ice (i.e., iceberg) fluxes. To predict potential ice sheet-ocean-climate feedbacks, we must know the partitioning of freshwater fluxes from Greenland, including the conversion of icebergs to liquid (i.e., meltwater) fluxes within glacial fjords. Here we use repeat ~0.5 m-resolution satellite images from two major fjords to provide the first observation-based estimates of the meltwater flux from the dense matrix of floating ice called mélange. We find that because of its expansive submerged area (>100 km^2) and rapid melt rate (~0.1–0.8 m d^{-1}), the ice mélange meltwater flux can exceed that from glacier surface and submarine melting. Our findings suggest that iceberg melt within the fjords must be taken into account in studies of glacial fjord circulation and the impact of Greenland melt on the ocean.

1. Introduction

The freshwater flux from the Greenland Ice Sheet into surrounding glacial fjords and ocean basins increased from ~750 $km^3\,yr^{-1}$ in the 1960s–1980s to ~1000 $km^3\,yr^{-1}$ in the 2000s [*Bamber et al*., 2012; *Lenaerts et al*., 2015] and is projected to continue to increase in the future [*Fürst et al*., 2015]. At the ice sheet margins, the partitioning of this flux into liquid (i.e., surface meltwater runoff and submarine meltwater fluxes) and solid (i.e., iceberg discharge) components is dictated by the glacier geometry and climate regime and varies around Greenland [*Bamber et al*., 2012; *Enderlin et al*., 2014]. Regional or global ocean models, however, do not resolve the fjords and typically prescribe the freshwater flux from Greenland as a boundary condition on the continental shelf [e.g., *Boning et al*. [2016]]. In translating a freshwater flux from the ice sheet margin to the continental shelf margin, however, one must take into account the conversion from solid to liquid that occurs due to iceberg melt within the fjords. The extent of this solid-to-liquid conversion is largely unknown, though a recent data-based study from Sermilik Fjord, a major glacial fjord in SE Greenland, suggests that iceberg melt may constitute a substantial fraction of the liquid freshwater export from the fjord during the summer [*Jackson and Straneo*, 2016]. Given that spatial variations in Greenland freshwater fluxes into the ocean influence the modeled impact of glacier mass loss on the thermohaline ocean circulation [*van den Berk and Drijfhout*, 2014; *Lenaerts et al*., 2015; *Luo et al*., 2016], it is important to accurately represent the freshwater fluxes around Greenland's coastal perimeter in global ocean models. Similarly, studies of fjord circulation and feedbacks between glacier mass loss and heat delivery to glacier termini have largely ignored the contribution of iceberg melt *within* the fjords as a driver of fjord circulation [*Carroll et al*., 2015; *Gladish et al*., 2015]. This in turn has implications for our ability to understand oceanic forcing of glaciers. Thus, understanding the extent to which the solid ice discharge is converted into liquid freshwater inside the fjords is important for studies of both ocean-driven melting of Greenland's glaciers and the impact of Greenland's melt on the global ocean.

For many glacial fjords, the movement of icebergs away from the terminus is retarded by the presence of an ice mélange, a seasonal to semipermanent matrix of icebergs and sea ice [*Amundson et al*., 2010; *Howat et al*., 2010; *Moon et al*., 2015], resulting in a lag of up to several months between an iceberg's initial detachment and its eventual discharge into the adjacent ocean basin [*Sutherland et al*., 2014]. While transiting fjords, icebergs can melt at rates of up to tens of centimeters per day below the waterline [*Enderlin and Hamilton*, 2014] releasing freshwater. The rate of iceberg mass loss due to this submarine melting (i.e., the total instantaneous

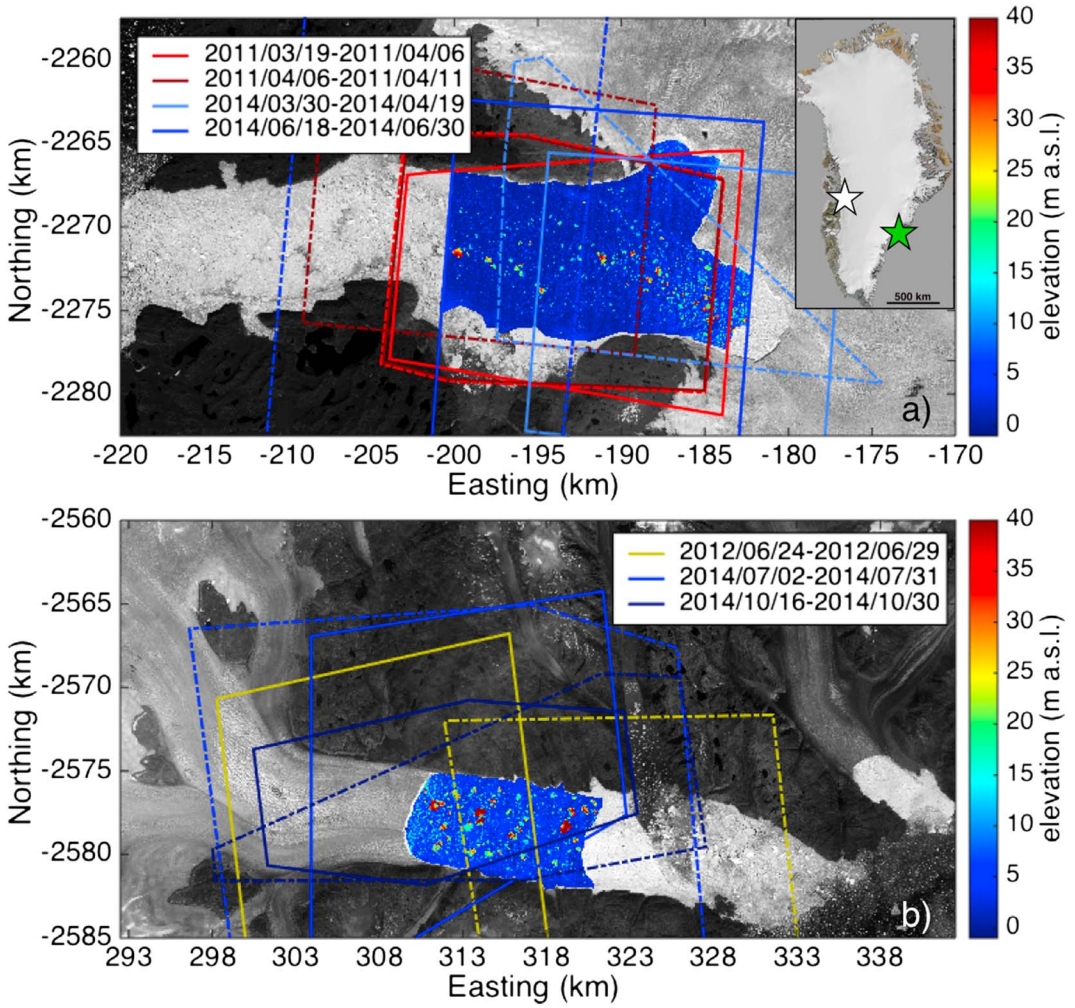

Figure 1. Spatial extent of ice mélange and DEM coverage. (a) Panchromatic Landsat 8 image of Ilulissat Isfjord on 3 July 2014 overlain by the mélange DEM from 18 June 2014. (b) Panchromatic Landsat 8 image of Sermilik Fjord on 29 July 2014 overlain by the mélange DEM from 31 July 2014. Mélange freeboard is indicated by the colorbars. Polygons show DEM footprints, with solid (dashed) lines indicating the first (second) date in each pair. In the inset Greenland map, white and green stars mark Ilulissat Isfjord and Sermilik Fjord, respectively.

meltwater flux from all icebergs present in the ice mélange), hereafter referred to as the iceberg meltwater flux or IMF, varies as a function of the area-averaged melt rate and submerged ice area, with a faster melt rate and/or larger submerged area corresponding to larger freshwater fluxes. The total iceberg mass loss also varies with the icebergs' residence time in the fjord (i.e., for fjords with expansive ice mélange, characterized by long residence times, the solid ice flux to the adjacent ocean is likely to be considerably reduced with respect to the iceberg discharge). Thus, iceberg melting is potentially both a significant source of liquid freshwater export from the fjords and an important sink for oceanic heat in glacial fjords.

Here we present the first estimates of iceberg melt within the ice mélange in two of Greenland's largest glacial fjords. Our estimates are derived from a remote sensing analysis of repeat digital elevation models (DEMs) produced using ~0.5 m-resolution satellite images [*Enderlin and Hamilton*, 2014]. Ilulissat Isfjord in West Greenland is fed by Jakobshavn Isbræ, and Sermilik Fjord in the southeast (Figure 1) is fed by Helheim Glacier, two of Greenland's most prolific iceberg producers [*Enderlin et al.*, 2014]. Both fjords contain large ($>1\,km^2$) and deep-drafted icebergs embedded within an expansive semipermanent ice mélange (extent $>175\,km^2$ and $\geq 50\,km^2$, respectively; Table S1 in the supporting information). Recent work has shown that these fjords also contain relatively warm (>2°C) subsurface water masses that deliver heat to the glaciers [*Straneo et al.*, 2011; *Gladish et al.*, 2015].

2. Data and Methods

2.1. Overview

The meltwater flux from an individual iceberg can be estimated directly from the difference in iceberg surface elevations extracted from repeat DEMs (see *Enderlin and Hamilton* [2014] and below). In principal, the DEM-differencing approach could be applied directly to the ice mélange if all icebergs could be identified or the mélange composition was identical in repeat DEMs. In practice, thousands of icebergs are constantly entering (via calving) and exiting the mélange (via drifting and melting), causing variations in mélange composition. Therefore, we use the alternative approach briefly described below. Additional details are presented in the following sections.

To estimate the IMF, we first use the DEM-differencing method to extract meltwater fluxes for a subset of icebergs in repeat DEMs. From this subset, we derive empirical relationships between iceberg meltwater fluxes and submerged areas (Figure S1) and drafts (Figure 2), yielding estimates of melt rates (i.e., meltwater flux divided by submerged area, $\dot{m}$). Next we estimate the draft of all pixels in the DEMs assuming hydrostatic equilibrium and divide the observed draft range into a series of M draft bins (each characterized by mean draft d_i, for $i = 1{:}M$). The IMF for each DEM date can then be expressed as the sum of the meltwater flux from icebergs within each draft bin as follows:

$$\mathrm{IMF} = \sum_{i=1}^{M} \dot{m}(d_i) A(d_i) N(d_i), \tag{1}$$

where $\dot{m}(d_i)$ is the melt rate, $A(d_i)$ is the submerged area, and $N(d_i)$ is the number of icebergs of draft d_i observed in the mélange. To obtain $N(d_i)$ for each DEM, we first sum the number of pixels in each draft bin then convert these draft distributions into iceberg size distributions (i.e., the number of icebergs in each draft bin) using characteristic iceberg aspect ratios extracted from the DEMs (Figure 3). We then extrapolate our iceberg size distributions to account for icebergs in the mélange that are outside the DEM. Finally, we estimate the submerged iceberg area for each draft bin and calculate the IMF using equation (1) (Figure 4).

2.2. Iceberg Melt Rates

To estimate melt rates (meters of ice ablated per day), we apply a DEM-differencing approach to a subset of (7–23) large icebergs that are identifiable in repeat WorldView satellite images following the procedures in *Enderlin and Hamilton* [2014]. DEMs of the fjord surface are constructed using the NASA Ames Stereo Pipeline [*Shean et al.*, 2016]. The DEMs are coregistered using open water elevations so that iceberg elevations are given with respect to sea level (i.e., freeboard) at the time of image acquisition. The change in freeboard is extracted from the DEMs, then converted to a volume change estimate under the assumption of hydrostatic equilibrium. After accounting for volume change due to subaerial melt using a positive degree-day approach [see *Enderlin and Hamilton*, 2014], we multiply the ice volume change by the density ratio between ice and water and divide by the time between DEM dates to yield estimates of the average submarine meltwater flux over that period.

In this study, we lump together lateral and basal melting and estimate the area-averaged melt rate for each iceberg as the volume change in time (i.e., meltwater flux) divided by the sum of the submerged lateral and bottom surface areas of a cylinder [see *Enderlin and Hamilton*, 2014]. We find that average iceberg melt rate per unit area can be empirically expressed as a function of the submerged area (Figure S1) or, alternatively, of iceberg draft (Figure 2) using a piecewise linear fit. The use of piecewise linear fits is necessary to account both for the high meltwater fluxes observed for deep-drafted icebergs and the small, but nonzero, melt rates observed for icebergs with a mean draft of less than ~150 m (Figure 2 and Table S1, columns 6–8). The pronounced increase in iceberg melt rate below ~150 m depth is consistent with the observed contrast in water temperatures and salinities: cold and fresh polar water (PW) in the upper ~150 m and overly warm and salty Atlantic water (AW) in both fjords [*Straneo et al.*, 2010, 2011; *Gladish et al.*, 2015; *Mernild et al.*, 2015].

2.3. Submerged Areas

To evaluate the IMF using equation (1), we have to estimate the distribution of icebergs of varying drafts (and hence submerged area) in the mélange. To do this, we first extract the freeboard of all mélange pixels in each DEM and estimate their draft under the assumption of hydrostatic equilibrium. We then compute the draft distribution, i.e., we parse the pixels into draft bins and sum the number of pixels in each draft bin, $n(d_i)$. Next, we estimate the number of icebergs in each draft bin ($N(d_i)$ in equation (1)) as

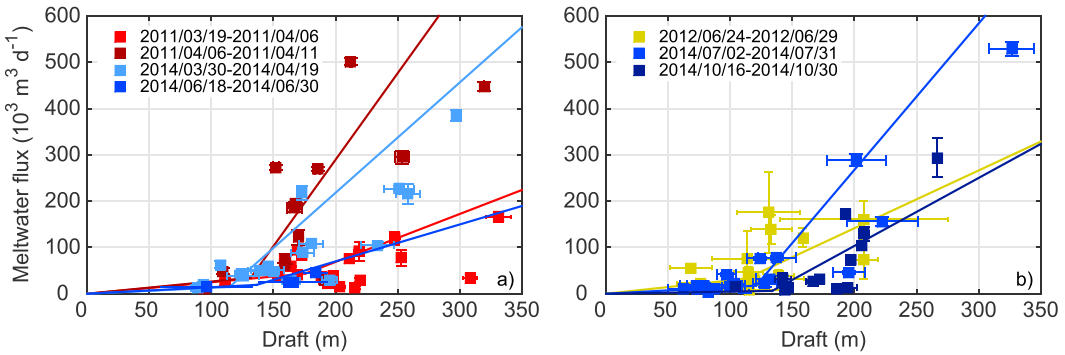

Figure 2. Iceberg meltwater flux versus mean draft for (a) Ilulissat and (b) Sermilik fjords. Horizontal error bars indicate the range in mean draft for the two observation dates, and vertical error bars account for elevation, area, density, and surface meltwater flux uncertainties. The apparent lack of error bars indicates that uncertainties are small and obscured by symbols. The trend lines are projected from Figure S1. Symbol and line colors distinguish observation periods.

$$N(d_i) = \frac{a \times n(d_i)}{\pi \left[\frac{1}{2} W(d_i)\right]^2}, \tag{2}$$

where a is the pixel resolution (m^2) and $W(d_i)$ is the average width of an iceberg in the ith bin (m). In equation (2), the numerator is the mélange extent occupied by all icebergs in the draft bin (m^2) and the denominator is

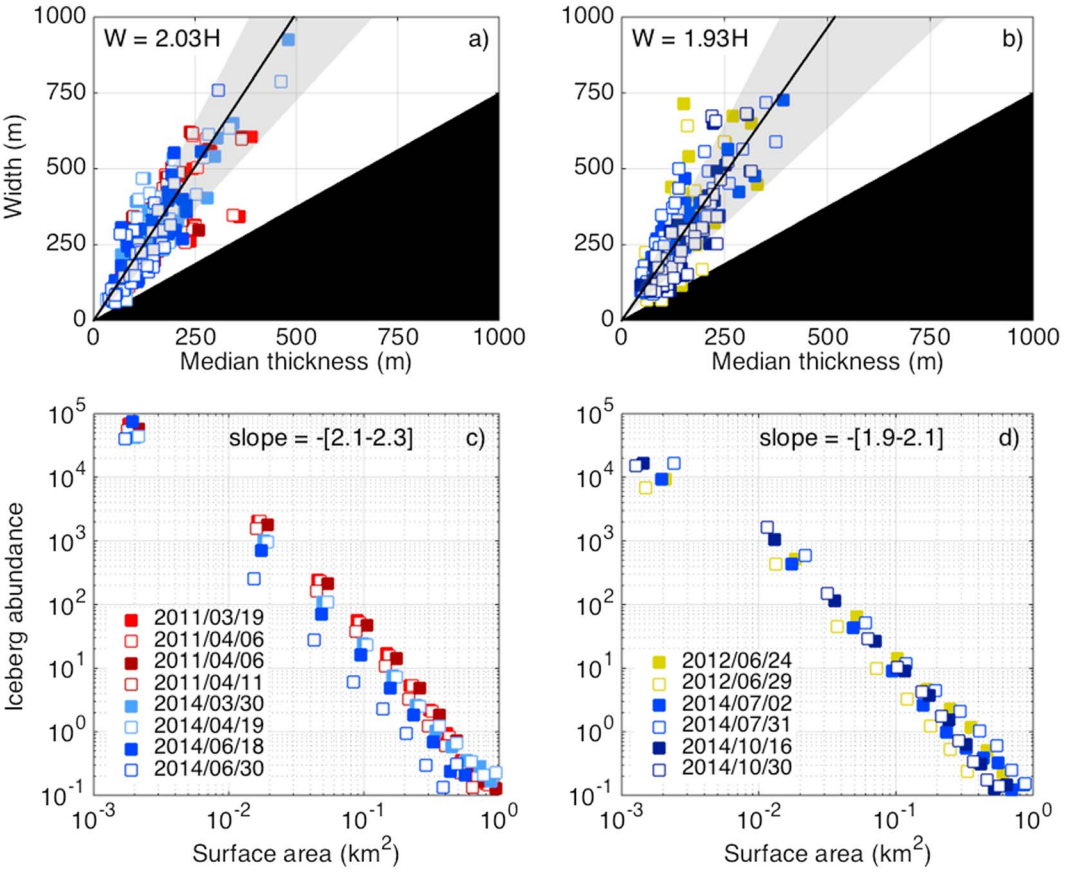

Figure 3. Iceberg aspect ratios and size distributions for (left column) Ilulissat and (right column) Sermilik fjords. (a, b) Aspect ratios for 40 representative icebergs for each DEM date. The black line and shaded gray region indicate the mean aspect ratio and one standard deviation uncertainty envelope. Icebergs with aspect ratios in the black region in the lower right corner of each subplot would spontaneously capsize [*Burton et al.*, 2012]. (c, d) Size distributions inferred from aspect ratios and freeboard observations. The legends in Figures 3c and 3d also pertain to Figures 3a and 3b, respectively.

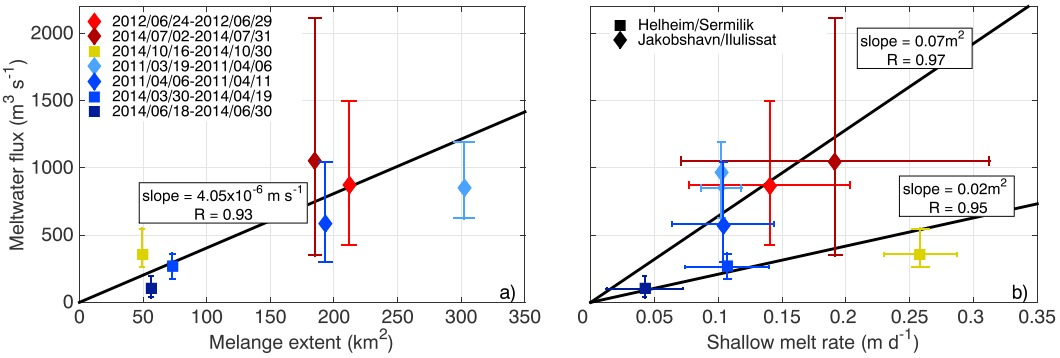

Figure 4. IMF plotted against (a) mélange extent and (b) shallow melt rates. Observation dates are distinguished by color, and fjords are distinguished by symbol. The trend line in Figure 4a is fit to the combined data sets. Trend lines in Figure 4b are shown for each fjord.

the average extent of an individual iceberg in that same bin (m^2 per iceberg). To solve for the denominator in equation (2), we compute the width and mean thickness (i.e., freeboard + draft) for 40 icebergs spanning the full range of sizes within the mélange and calculate the average width-to-thickness (i.e., aspect) ratio, ε, for each DEM date. We find that for both fjords, icebergs are roughly twice as wide as they are thick (Figures 3a and 3b). We then estimate the mean iceberg thickness for each bin, $H(d_i)$, and calculate the width as $W(d_i) = \varepsilon H(d_i)$. Using this approach, peaks in freeboard >50 m in the largest icebergs are erroneously identified as fractions of very large (i.e., >1 km^2) icebergs that exceed the observed maximum iceberg size. To account for such misidentifications, we reassign these pixels to the largest size bin. Finally, assuming a cylindrical submerged geometry, the submerged iceberg areas are estimated for each bin ($A(d_i)$ in equation (1)).

2.4. Mélange Meltwater Flux

To estimate the IMF from the portion of the mélange covered by each DEM, we solve equation (1) for each draft bin using shallow (deep) melt rates for drafts less than (greater than) 115–176 m, depending on the DEM date range (Table S1). The DEMs do not cover the entire mélange extent (see Figure 1), however, and the IMF outside the DEMs must be added to the estimates from equation (1). To estimate the IMF outside the DEMs, we first extract the draft distribution and mean draft for 1 km long boxes that span the width of the mélange (Figure S2). After applying linear and quadratic functions to the draft profiles, we use the fit with the highest correlation coefficient to assess whether iceberg size varies significantly with distance from the terminus due to melting and fragmentation. For fits with $R^2 < 0.7$ (all Sermilik dates) we measure the full mélange extents in nearly contemporaneous Landsat panchromatic images and use the ratios between the entire mélange extents and DEM extents to scale up the IMF estimates. For significant along-fjord changes in iceberg size (i.e., $R^2 > 0.7$), we use nearly contemporaneous Landsat images to measure the spatial extent and along-fjord distance from the terminus for each patch of mélange that fall outside the DEMs. The iceberg size distribution in each mélange patch is then estimated from the nearest box in the nearly contemporaneous DEM, taking into account differences in the extent of the mélange patch and the box. The iceberg abundances, $N(d_i)$, are then adjusted to account for icebergs outside the DEMs, and the IMFs for the entire ice mélange are calculated using equation (1). Uncertainties associated with the extrapolation, submerged iceberg area estimates, and melt rates are discussed in the supporting information.

3. Results and Discussion

Using our remote sensing approach, we find that melt rates for the two fjords are similar, with shallow-drafted (deep-drafted) iceberg melt rates ranging from ~0.11 to 0.21 m d^{-1} (~0.18–0.83 m d^{-1}) and ~0.05 to 0.29 m d^{-1} (0.31–0.67 m d^{-1}) for Ilulissat and Sermilik fjords, respectively (Table S1, columns 7–8). On average, melt rates for deep-drafted icebergs are 3 times larger than the melt rates for shallow icebergs, with significant differences (i.e., difference exceeds combined uncertainties) in melt rates between shallow- and deep-drafted icebergs for four of seven observation periods. Significant temporal variations occur on weekly to interannual time scales, consistent with the idea that melt rates depend on multiple factors, including

water temperatures and iceberg and current velocities [*Bigg et al*., 1997], which have been observed to vary over a range of time scales [e.g., *Jackson et al*. [2014]].

In regard to iceberg size, we find comparable aspect ratios for both fjords (Figures 3a and 3b and Table S1, column 9) that suggest that icebergs in the mélange are highly stable (i.e., aspect ratio $\gg 0.75$) [*Weeks and Mellor*, 1978; *Burton et al*., 2012]. This is potentially due to a similar calving style for both glaciers (e.g., *Amundson et al*. [2010] for Jakobshavn and *Murray et al*. [2015] for Helheim). Likewise, the iceberg size distributions are similar for both fjords and can be reasonably approximated as a power law distribution with an exponent of -2.1 (Figures 3c and 3d), in contrast with the $-3/2$ exponent observed for Antarctic icebergs [*Tournadre et al*., 2015]. Accordingly, we estimate that at any moment there are >10,000 growlers confined to the PW layer (Figure S3) that are unresolved from automated iceberg identification methods [e.g., *Foga et al*., 2014] but are captured by our approach.

Our DEM analysis suggests that submarine melting occurs over a vast submerged mélange area. Estimated submerged mélange areas range from 466 to 685 km^2 in Ilulissat Isfjord and 132 to 261 km^2 in Sermilik Fjord (Table S1, column 10). These estimates exceed the submerged terminus areas of Jakobshavn Isbræ and Helheim Glacier (~9–27 km^2 and ~5–15 km^2, respectively) by at least an order of magnitude (see supporting information). Variations in the submerged mélange area between observation dates are driven primarily by changes in the linear extent of the mélange. We also find that submerged mélange area is highly sensitive to small variations in aspect ratio, which presumably reflect variations in calving style, with larger aspect ratios corresponding to smaller submerged area estimates. To demonstrate this relationship, consider 31 July and 30 October 2014 in Sermilik Fjord (Table S1): the mélange extent is similar (~82 km^2), but in July the mélange is composed of wider icebergs and the estimated submerged area is ~56 km^2 smaller than in October. The dependence of the submerged mélange area on mélange extent and aspect ratio suggests that variations in both the volume and style of iceberg calving influence the submerged mélange area. In the absence of expansive floating ice tongues, we expect that the submerged mélange area considerably exceeds the submerged glacier area in the iceberg-congested fjords spanning the Greenland ice sheet periphery.

The derived IMFs range from 678–1346 $m^3 s^{-1}$ in Ilulissat Isfjord to 126–494 $m^3 s^{-1}$ in Sermilik Fjord (Figure 4 and Table S1, column 11). Temporal variations in the IMF within each fjord are strongly correlated with differences in melt rates for shallow-drafted icebergs, growlers, and sea ice ($R \approx 0.96$). This finding makes intuitive sense because small icebergs dominate the mélange in terms of abundance and submerged area and have the highest submerged area-to-volume ratio (up to 0.11 m^2/m^3). We note that for individual fjords, the correlation between mélange extent and IMF is not statistically significant owing to the sparse observational record, but when the observations for both fjords are combined, we find that variations in IMF are significantly correlated (i.e., $p < 0.05$, $R = 0.97$) with differences in mélange extent.

Although our observations only provide snapshot estimates of the IMF from the mélange in these two fjords, the relatively high melt rates that we observe and the year-round persistence of ice mélange suggest that their IMFs should remain on the order of hundreds of cubic meters per second throughout the year. In contrast, surface runoff fluxes at the glacier margins have strong seasonal variability, from near-zero fluxes during October–April to a summer peak of ~900 $m^3 s^{-1}$ for Ilulissat [*Mernild et al*., 2015] and ~1000 $m^3 s^{-1}$ for Sermilik [*Andersen et al*., 2010]. Furthermore, seasonal variations in surface runoff likely drive variations in the rate of submarine melting along the submerged glacier termini [*Sciascia et al*., 2013], enhancing seasonality in the glacier meltwater flux. Estimates of glacier submarine melt rates are highly uncertain, but recent studies suggest that when runoff is near zero (i.e., October–April), melt rates along the submerged glacier termini are similar to iceberg melt rates [*Enderlin and Hamilton*, 2014]. In summer months, glacier submarine melt rates can reach up to 3.5 $m\,d^{-1}$ where buoyant meltwater plumes are in contact with termini [*Fried et al*., 2015; *Slater et al*., 2015]. Applying this melt rate over the entire submerged areas at both glaciers gives upper bound estimates for summertime glacier submarine meltwater fluxes of ~200 $m^3 s^{-1}$ and ~400 $m^3 s^{-1}$ for Helheim and Jakobshavn, respectively; for comparison, the IMFs range from 126 to 494 $m^3 s^{-1}$ and 678 to 1346 $m^3 s^{-1}$. Thus, our analysis suggests that IMFs constitute a nonnegligible fraction of the total freshwater input to iceberg-congested glacial fjords in summer. Moreover, given that the submerged terminus areas for these glaciers are estimated to be at least an order of magnitude smaller than their respective submerged mélange areas (see supporting information), we expect that the IMF will dominate the freshwater budget of Greenland's glacial fjords containing ice mélange in the nonsummer months.

Melting of icebergs while they are embedded in mélange leads to a reduction in the flux of solid ice exported from glacial fjords. To derive first-order estimates of this fractional reduction of ice discharge, we scale our IMFs using representative iceberg residence times for each fjord [*Sutherland et al*., 2014] and divide by the solid ice discharge. Residence times are obtained from GPS trackers deployed on large icebergs during summer 2014 in Ilulissat and 2012/2014 in Sermilik [*Sutherland et al*., 2014], and ice discharge is from *Enderlin et al*. [2014] (see supporting information). Over the average 20–day residence time for icebergs in the Ilulissat Fjord mélange, submarine melting reduces their volume by 10–24%. The reduction is larger in Sermilik Fjord (12–49%), where the average iceberg residence time is 51 days. These estimates account for temporal variations in the IMF between observation dates, including early melt-out of the smallest icebergs, but do not account for potential variations in residence time. Additionally, we do not account for mass loss that will occur after the icebergs exit the mélange and traverse the open fjord waters, where icebergs may melt at markedly different rates. Nevertheless, our results suggest that 50% or more of solid ice mass may be converted to liquid freshwater before icebergs enter the open ocean, which is consistent with the 20–30% reduction in iceberg volume estimated for Kangerdlugssuaq Fjord (~350 km NNE of Sermilik Fjord) using a modeling approach [*Mugford and Dowdeswell*, 2010].

4. Conclusion

Iceberg discharge from the Greenland ice sheet has increased over the last several decades, accounting for up to half of the observed mass loss [*Enderlin et al*., 2014], yet the fate of these icebergs and their impact on fjord and ocean circulation have been largely ignored. Here we use repeat very high resolution digital elevation models to show that iceberg meltwater fluxes are on the order of hundreds to thousands of cubic meters per second in Greenland's iceberg-congested fjords. For Ilulissat Isfjord and Sermilik Fjord, we find that mélange meltwater fluxes dominate each fjord's freshwater budget for the majority of the year (IMFs of 678–1346 $m^3 s^{-1}$ and 126–494 $m^3 s^{-1}$, respectively, compared to peak glacier meltwater fluxes of ~1200–1300 $m^3 s^{-1}$). Although we presently do not have the observational data required to estimate IMFs for other fjords, the strong dependence on mélange submerged area demonstrated here and the pervasiveness of winter mélange suggests that ice mélange meltwater fluxes likely dominate freshwater fluxes to Greenland's iceberg-congested fjords in winter months. Where mélange persists year-round, our data suggest that mélange meltwater fluxes are nontrivial in the summer months as well.

The weeks-long residence times of icebergs trapped in the mélange in Ilulissat and Sermilik fjords lead to large cumulative iceberg meltwater fluxes that likely play an important role in the formation of the thick layer of cold and fresh near-surface water found close to Greenland's outlet glaciers [*Straneo et al*., 2011; *Gladish et al*., 2015]. Thus, it is imperative that iceberg meltwater fluxes are taken into account in analyses of hydrographic observations acquired near fjord mouths and are included as a forcing term in modeling studies of glacial fjords. Furthermore, these large cumulative fluxes are associated with a ~10–50% reduction in solid ice volume between the glacier terminus and open ocean that should be accounted for when imposing solid and liquid freshwater flux boundary conditions in large-scale ocean models.

Acknowledgments

Thank you to two anonymous reviewers and Kristin Schild for their insightful recommendations, particularly in regard to the methods description. Ice mélange melt rates, meltwater fluxes, and size distributions can be extracted from Table S1 and the figures in the manuscript and supporting information. More detailed observational data can be obtained by contacting the corresponding author (ellyn.enderlin@gmail.com).

References

Andersen, M. L., et al. (2010), Spatial and temporal melt variability at Helheim Glacier, East Greenland, and its effect on ice dynamics, *J. Geophys. Res.*, *115*, F04041, doi:10.0129/2010JF001760.

Amundson, J. M., M. Fahnestock, M. Truffer, J. Brown, and M. P. Lüthi (2010), Ice mélange dynamics and implications for terminus stability, Jakobshavn Isbræ, Greenland, *J. Geophys. Res.*, *115*, F01005, doi:10.1029/2009JF001405.

Bamber, J., M. van den Broeke, J. Ettema, J. Lenaerts, and E. Rignot (2012), Recent large increases in freshwater fluxes from Greenland in the North Atlantic, *Geophys. Res. Lett.*, *39*, L19501, doi:10.1029/2012GL052552.

Bigg, G. R., M. R. Wadley, D. P. Stevens, and J. A. Johnson (1997), Modelling the dynamics and thermodynamics of icebergs, *Cold Reg. Sci. Technol.*, *26*, 113–135.

Boning, C. W., E. Behrens, A. Biastoch, K. Getzlaff, and J. L. Bamber (2016), Emerging impact of Greenland meltwater on deepwater formation in the North Atlantic Ocean, *Nat. Geosci.*, *9*, 523–528, doi:10.1038/NGEO2740.

Burton, J. C., J. M. Amundson, D. S. Abbot, A. Boghosian, L. M. Cathles, S. Correa-Legisos, K. N. Darnell, N. Guttenberg, D. M. Holland, and D. R. MacAyeal (2012), Laboratory investigations of iceberg capsize dynamics, energy dissipation and tsunamigenesis, *J. Geophys. Res.*, *117*, F01007, doi:10.1029/2011JF002055.

Carroll, D., D. A. Sutherland, E. L. Shroyer, J. D. Nash, G. Catania, and L. A. Stearns (2015), Modeling turbulent subglacial meltwater plumes: Implications for fjord-scale buoyancy-driven circulation, *J. Phys. Ocean.*, *45*, 2169–2185, doi:10.1175/JPO-D-15-0033.1.

de Juan, J., et al. (2010), Sudden increase in tidal response linked to calving and acceleration at a large Greenland outlet glacier, *Geophys. Res. Lett.*, *37*, L12501, doi:10.1029/2010GL043289.

Enderlin, E. M., and G. S. Hamilton (2014), Estimates of iceberg submarine melting from high-resolution digital elevation models: Applications to Sermilik Fjord, East Greenland, *J. Glaciol.*, *60*(224), 1084–1092, doi:10.3189/2014GoJ14J085.

Enderlin, E. M., I. M. Howat, S. Jeong, M.-J. Noh, J. van Angelen, and M. R. van den Broeke (2014), An improved mass budget for the Greenland ice sheet, *Geophys. Res. Lett.*, *41*, 866–872, doi:10.1002/2013GL059010.

Foga, S., L. A. Stearns, and C. J. van der Veen (2014), Application of satellite remote sensing techniques to quantify terminus and ice mélange behavior at Helheim Glacier, East Greenland, *Mar. Technol. Soc. J.*, *48*(5), 81–91.

Fried, M. J., G. A. Catania, T. C. Bartholomaus, D. Duncan, M. Davis, L. A. Stearns, J. Nash, E. Shroyer, and D. Sutherland (2015), Distributed subglacial discharge drives significant submarine melt at a Greenland tidewater glacier, *Geophys. Res. Lett.*, *42*, 9328–9336, doi:10.1002/2015GL065806.

Fürst, J. J., H. Goelzer, and P. Huybrechts (2015), Ice-dynamic projections of the Greenland ice sheet in response to atmospheric and oceanic warming, *The Cryo.*, *9*, 1039–1062, doi:10.2194/tc-9-1039-2015.

Gladish, C. V., D. M. Holland, A. Rosing-Asvid, J. W. Behrens, and J. Boje (2015), Oceanic boundary conditions for Jakobshavn Glacier. Part I: Variability and renewal of Ilulissat Icefjord Waters, 2001–14, *J. Phys. Ocean.*, *45*, 3–32, doi:10.1175/JPO-D-14-0044.1.

Howat, I. M., J. E. Box, Y. Ahn, A. Herrington, and E. M. McFadden (2010), Seasonal variability in the dynamics of marine-terminating outlet glaciers in Greenland, *J. Glaciol.*, *56*(198), 601–613.

Jackson, R. H., and F. Straneo (2016), Heat, salt, and freshwater budgets for a glacial fjord in Greenland, *J. Phys. Ocean.*, doi:10.1175/JPO-D-15-0134.

Jackson, R. H., F. Straneo, and D. A. Sutherland (2014), Externally forced fluctuations in ocean temperature at Greenland glaciers in non-summer months, *Nat. Geosci.*, *7*, 503–508, doi:10.1038/NGEO2186.

Joughin, I., B. E. Smith, D. A. Shean, and D. Floricoiu (2014), Further summer speedup of Jakobshavn Isbræ, *The Cryo.*, *8*, 209–214, doi:10.5194/tc-8-209-2014.

Lenaerts, J. T. M., D. Le Bars, L. van Kampenhout, M. Vizcaino, E. M. Enderlin, and M. R. van den Broeke (2015), Representing Greenland ice sheet freshwater fluxes in climate models, *Geophys. Res. Lett.*, *42*, 6373–6381, doi:10.1002/2015GL064738.

Luo, H., R. M. Castelao, A. K. Rennermalm, M. Tedesco, A. Bracco, P. L. Yager, and T. L. Mote (2016), Oceanic transport of surface meltwater from the southern Greenland ice sheet, *Nat. Geosci.*, *9*, 528–532, doi:10.1038/NGEO2708.

Mernild, S. H., D. M. Holland, D. Holland, A. Rosing-Asvid, J. C. Yde, G. E. Liston, and K. Steffen (2015), Freshwater flux and spatiotemporal simulated runoff variability into Ilulissat Icefjord, West Greenland, linked to salinity and temperature observations near tidewater glacier margins obtained using instrumented ringer seals, *J. Phys. Ocean.*, *45*, 1426–1445, doi:10.1175/JPO-D-14.0217.1.

Moon, T., I. Joughin, and B. Smith (2015), Seasonal to multiyear variability of glacier surface velocity, terminus position, and sea ice/ice mélange in northwest Greenland, *J. Geophys. Res. Earth Surf.*, *120*, 818–833, doi:10.1002/2015JF003494.

Mugford, R. I., and J. A. Dowdeswell (2010), Modeling iceberg-rafted sedimentation in high-latitude fjord environments, *J. Geophys. Res.*, *115*, F03024, doi:10.1029/2009JF001564.

Murray, T., N. Selmes, T. D. James, S. Edwards, I. Martin, T. O'Farrell, R. Aspey, I. Rutt, M. Nettles, and T. Baugé (2015), Dynamics of glacier calving at the ungrounded margin of Helheim Glacier, southeast Greenland, *J. Geophys. Res. Earth Surf.*, *120*, 964–982, doi:10.1002/2015JF003531.

Sciascia, R., F. Straneo, C. Cenedese, and P. Heimbach (2013), Seasonal variability of submarine melt rate and circulation in an East Greenland fjord, *J. Geophys. Res. Oceans*, *118*, 2492–2506, doi:10.1002/jgrc.20142.

Shean, D. A., O. Alexandrov, Z. M. Moratto, B. E. Smith, I. R. Joughin, C. Porter, and P. Morin (2016), An automated, open-source pipeline for mass production of digital elevation models (DEMs) from very-high-resolution commercial stereo satellite imagery, *ISPRS J. Photogram. Remote Sens.*, *116*, 101–117, doi:10.1016/j.isprsjprs.2016.03.012.

Slater, D. A., P. W. Nienow, T. R. Cowton, D. N. Goldberg, and A. J. Sole (2015), Effect of near-terminus subglacial hydrology on tidewater glacier submarine melt rates, *Geophys. Res. Lett.*, *42*, 2861–2868, doi:10.1002/2014GL062494.

Straneo, F., R. G. Curry, D. A. Sutherland, G. S. Hamilton, C. Cenedese, K. Våge, and L. A. Stearns (2011), Impacts of fjord dynamics and glacial runoff on the circulation near Helheim Glacier, *Nat. Geosci.*, *4*, 322–327, doi:10.1038/NGEO1109.

Straneo, F., G. S. Hamilton, D. A. Sutherland, L. A. Stearns, F. Davidson, M. O. Hammill, G. B. Stenson, and A. Rosing-Asvid (2010), Rapid circulation of warm subtropical waters in a major fjord in East Greenland, *Nat. Geosci.*, *3*, 182–186, doi:10.1038/NGEO764.

Sutherland, D. A., G. E. Roth, G. S. Hamilton, S. H. Mernild, L. A. Stearns, and F. Straneo (2014), Quantifying flow regimes in a Greenland glacial fjord using iceberg drifters, *Geophys. Res. Lett.*, *41*, 8411–8420, doi:10.1002/2014GL062256.

Tournadre, J., N. Bouhier, F. Girard-Ardhuin, and F. Rémy (2015), Antarctic icebergs distributions 1992–2014, *J. Geophys. Res. Oceans*, *120*, doi:10.1002/2015JC-11178.

van den Berk, J., and S. S. Drijfhout (2014), A realistic freshwater forcing protocol for ocean-coupled climate models, *Ocean Modell.*, *81*, 36–48, doi:10.1016/j.ocemod.2014.07.003.

Weeks, W. F. and M. Mellor (1978), Some elements of iceberg technology, *Proceedings of the First Conference on Iceberg Utilization for Freshwater Production*, 45-98.